UCRL-ID-140697

Calculation of ^{239}Pu(n,2n) cross section by the subtraction and the ratio methods

P. Navratil and D.P. McNabb

September 28, 2000

U.S. Department of Energy

Lawrence
Livermore
National
Laboratory

Work performed under the auspices of the U. S. Department of Energy by the University of California Lawrence Livermore National Laboratory under Contract W-7405-Eng-48.

Calculation of ^{239}Pu(n,2n) cross section by the subtraction and the ratio methods

P. Navratil* and D. P. McNabb

University of California, Lawrence Livermore National Laboratory, P. O. Box 808, Livermore, CA 94551

Abstract

The ^{239}Pu(n,2n) and the ^{235}U(n,2n) cross section are estimated by applying unitarity in several approaches: a subtraction method and also by using a ratio approach that relates the above cross sections to the ^{238}U(n,2n) cross section and the ^{239}Pu(n,2n) cross section to the ^{235}U(n,2n) cross section, respectively. Also, a self-consistent, simultaneous analysis of the cross section data of four nuclei, ^{239}Pu, ^{235}U, ^{238}U and ^{232}Th, was undertaken to evaluate the ^{239}Pu(n,2n) cross section at 11 MeV.

I. INTRODUCTION

There is an ongoing joint effort at the LLNL and the LANL to evaluate the ^{239}Pu(n,2n)^{238}Pu cross section. New experimental measurements have been carried out using the GEANIE detector to determine the partial cross sections for the ^{239}Pu(n,2nγ) reaction [1]. Nuclear theory modeling calculations are applied to these experimental results to determine the total cross section [2].

In this report we concentrate on a complementary evaluation of the ^{239}Pu(n,2n) cross section by relating available experimental cross sections using variations on unitarity arguments suggested by J. D. Anderson [3].

The subtraction approach to the evaluation of the (n,2n) cross sections for heavy nuclei balances the non-elastic cross section with the (n,n') and other open channel cross sections [4]. We apply a variation of this approach to evaluate the ^{239}Pu(n,2n)^{238}Pu cross section.

II. SUBTRACTION METHOD

Unitarity can be directly applied to relate the ^{239}Pu(n,2n) cross section to the non-elastic cross section obtained from the optical model, the experimental fission cross section and the experimental ^{239}Pu(n,n') cross section. The capture and charge-particle emission channels are assumed to be negligible. It is assumed that the ^{239}Pu(n,n') cross section is proportional

*ext 4-3725, L 414, e-mail navratil1@llnl.gov

to the measured ^{239}Pu(n,n'γ) cross section. The proportionality constant is evaluated from the difference of the reaction cross section and the fission cross section below the (n,2n) threshold. Thus, we use

$$\sigma^{239}_{(\mathrm{n,2n})}(E) = \sigma_{\mathrm{r-DI}}(E) - \sigma^{239}_{\mathrm{f}}(E) - \sigma^{239}_{(\mathrm{n,n'})}(E) \ . \tag{1}$$

Here, $\sigma_{\mathrm{r-DI}}$ is the non-elastic cross section equal to the reaction cross section minus the direct collective state excitation cross section. For $\sigma_{\mathrm{r-DI}}$ we use the Flap2.2 optical model potential calculated by F. Dietrich [5]. This potential was fitted to ^{238}U experimental data. The direct excitation to the 2^+ and 4^+ ground-state band states was subtracted. We assume that the error in determination of $\sigma_{\mathrm{r-DI}}$ is 3%. Also, we assume a simple scaling of the optical potential for nuclei of interest by a factor of $(A/238)^{\frac{2}{3}}$, i.e.,

$$\sigma^{A}_{\mathrm{r-DI}} = \sigma^{238}_{\mathrm{r-DI}}(A/238)^{\frac{2}{3}} \ . \tag{2}$$

The fission cross section $\sigma^{239}_{\mathrm{f}}$ is obtained from ENDL and we assume an error of 1.5% for this cross section. In Fig. 1 we present the reaction and fission cross sections.

The $\sigma^{239}_{(\mathrm{n,n'})}$ cross section we obtain from the assumption that it is proportional to a (n,n'γ) cross section measured experimentally [6,7]. We use then

$$\sigma^{239}_{(\mathrm{n,n'})}(E) = \alpha_\gamma \sigma^{239}_{(\mathrm{n,n'}\gamma)}(E) \ , \tag{3}$$

and the normalization factor α_γ is obtained from the condition

$$\sigma_{\mathrm{r-DI}}(E_{\mathrm{tr}}) - \sigma^{239}_{\mathrm{f}}(E_{\mathrm{tr}}) = \alpha_\gamma \sigma^{239}_{(\mathrm{n,n'}\gamma)}(E_{\mathrm{tr}}) \tag{4}$$

below (n,2n) threshold. The subscript at E_{tr} in Eq. (4) emphasizes that the energy is below the (n,2n) threshold.

We calculate the error of $\sigma^{239}_{(\mathrm{n,2n})}(E)$ under assumption that the reaction cross sections $\sigma_{\mathrm{r-DI}}$ appearing in Eq. (1) evaluated at different energies are independent. The same is assumed about the fission cross sections in Eq. (1) as well as the experimental cross sections $\sigma^{239}_{(\mathrm{n,n'}\gamma)}(E)$. Consequently, using the standard error propagation, the error of $\sigma^{239}_{(\mathrm{n,n'})}$ was calculated from the experimental error of $\sigma^{239}_{(\mathrm{n,n'}\gamma)}$ and from the error of α_γ as

$$\delta\sigma^{239}_{(\mathrm{n,n'})} = \sqrt{(\alpha_\gamma \delta\sigma^{239}_{(\mathrm{n,n'}\gamma)})^2 + (\sigma^{239}_{(\mathrm{n,n'}\gamma)}\delta\alpha_\gamma)^2} \ , \tag{5}$$

with

$$\delta\alpha_\gamma = \sqrt{(\delta\sigma_{\mathrm{r-DI}}/\sigma^{239}_{(\mathrm{n,n'}\gamma)})^2 + (\delta\sigma^{239}_{\mathrm{f}}/\sigma^{239}_{(\mathrm{n,n'}\gamma)})^2 + ((\sigma_{\mathrm{r-DI}} - \sigma^{239}_{\mathrm{f}})\delta\sigma^{239}_{(\mathrm{n,n'}\gamma)}/(\sigma^{239}_{(\mathrm{n,n'}\gamma)})^2)^2} \ . \tag{6}$$

The relations (4) and (6) are evaluated for several experimental measurements for energies in a range 0.6-1.6 MeV below the (n,2n) threshold that is at 5.6704 MeV for ^{239}Pu. The final α_γ and $\delta\alpha_\gamma$ are then obtained by averaging, i.e.,

$$\alpha_\gamma = \frac{1}{\omega}\sum_i \frac{1}{(\delta\alpha_{\gamma,i})^2}\alpha_{\gamma,i} \ , \tag{7a}$$

$$\omega = \sum_i \frac{1}{(\delta\alpha_{\gamma,i})^2} \ , \tag{7b}$$

$$\delta\alpha_\gamma = \frac{1}{\sqrt{\omega}} \ . \tag{7c}$$

The total number of the points in the sums in (7) varied from 3 to 7 depending on the size of the interval (0.6-1.6 MeV). However, the final results were only very weakly sensitive to this size. Eventually, to evaluate the error $\delta\sigma^{239}_{(\mathrm{n,2n})}(E)$ we use

$$\delta\sigma^{239}_{(\mathrm{n,2n})} = \sqrt{(\delta\sigma_{\mathrm{r-DI}})^2 + (\delta\sigma^{239}_{\mathrm{f}})^2 + (\delta\sigma^{239}_{(\mathrm{n,n'})})^2}\,. \tag{8}$$

We had four γ transition measurements available for ^{239}Pu, i.e., 227 keV $\frac{5}{2}^-$(505keV) $\rightarrow \frac{5}{2}^+$, 228 keV $\frac{5}{2}^+$(285keV) $\rightarrow \frac{7}{2}^+$, 278 keV $\frac{5}{2}^+$(285keV) $\rightarrow \frac{3}{2}^+$ and 154 keV $\frac{13}{2}^+$(318keV) $\rightarrow \frac{9}{2}^+$ [6]. The two γ transitions from the level $\frac{5}{2}^+$(285keV) are significantly stronger than the other two transitions are thus preferably used in our calculations. When applying formulas (3) and (4) we used the energies E at which the $\sigma_{(\mathrm{n,n'}\gamma)}$ were measured. The other cross sections were interpolated to these energies using natural cubic splines. As stated earlier, the energies E_i^{tr} were chosen from the measured $\sigma_{(\mathrm{n,n'}\gamma)}$ points in the range from 0.6 to 1.6 MeV below the (n,2n) threshold that is at 5.6704 MeV for ^{239}Pu. The evaluated (n,2n) cross section was not particularly sensitive to the extent of the range, although the overall error is reduced if a larger range is utilized. Number of points varied from 3 to 7. In Fig. 2 we show the $\sigma_{(\mathrm{n,n'}\gamma)}$ cross section corresponding to the sum of the two strong transitions, i.e., 228 keV and 278 keV.

In Fig. 3, we present the calculated (n,2n) ^{239}Pu cross section with its error obtained as described earlier in this Section. When we consider a sum of the 228 keV and 278 keV γ transitions in ^{239}Pu, at 11.37 MeV we obtain the (n,2n) cross section $\sigma^{239}_{(\mathrm{n,2n})} = 0.527 \pm 0.102$ b. At this energy, we have the following contributions from the individual cross sections: $\sigma_{\mathrm{r-DI}} = 2.992 \pm 0.090$ b, $\sigma_{\mathrm{f}} = 2.235 \pm 0.034$ b and $\sigma_{(\mathrm{n,n'})} = 0.230 \pm 0.034$ b. The dominant contribution to the error comes from the reaction cross section.

We performed the same analysis also for ^{235}U(n,2n) using the above formulas with 239 cross sections replaced by the corresponding 235 cross sections. We use $\sigma_{(\mathrm{n,n'}\gamma)}$ for the 129 keV γ transition $\frac{5}{2}^-$(129keV) $\rightarrow \frac{7}{2}^-$, see Fig. 4. In this evaluation we used the new $\sigma_{(\mathrm{n,n'}\gamma)}$ data that are free of the wraparound background up to 9.23 MeV [7]. We note that no wraparound background correction was applied for the energies above 9.23 MeV. Similarly, the ^{239}Pu transitions were not corrected for this background. We also note that the ^{235}U(n,2n) threshold is at 5.3206 MeV. The resulting cross section is presented in Fig. 5. At 11.23 MeV we obtained $\sigma^{235}_{(\mathrm{n,2n})} = 0.844 \pm 0.100$ b. This value is in good agreement with the Frehaut measurement at this energy.

The individual cross sections at 11 MeV are summarized in Table I.

III. RATIO METHOD

As there are experimental measurements of the ^{238}U(n,2n) cross section, we may relate those data to the cross section we are interested in by using, e.g.,

$$\sigma^{239}_{(\mathrm{n,2n})}(E) = \frac{\sigma^{239}_{\mathrm{r-DI}}(E) - \sigma^{239}_{\mathrm{f}}(E) - \sigma^{239}_{(\mathrm{n,n'})}(E)}{\sigma^{238}_{\mathrm{r-DI}}(E') - \sigma^{238}_{\mathrm{f}}(E') - \sigma^{238}_{(\mathrm{n,n'})}(E')}\sigma^{238}_{(\mathrm{n,2n})}(E') \equiv \frac{\sigma^{239}_{\mathrm{subtr}}(E)}{\sigma^{238}_{\mathrm{subtr}}(E')}\sigma^{238}_{(\mathrm{n,2n})}(E')\,. \tag{9}$$

In the above equation, we relate the energy E and E' by the differences in the (n,2n) thresholds for the two nuclei, i.e., $E' = E + E^{238}_{\mathrm{tr}} - E^{239}_{\mathrm{tr}}$. The non-elastic cross sections

$\sigma^{A}_{\text{r-DI}}$ in (9) are related by the relation (2). Thus, when calculating error propagation, the reaction cross sections in (9) that carry a dominant error, are dependent and the error partially cancels. In general, the overall error is then smaller than that obtained using the subtraction method of the previous section. To evaluate the errors we consider the other ^{239}Pu cross sections independent on the ^{238}U cross sections and use the following relations

$$\frac{\partial\sigma^{239}_{(\text{n,2n})}(E)}{\partial\sigma^{239}_{\text{r-DI}}(E)} = \frac{\sigma^{238}_{(\text{n,2n})}(E')}{\sigma^{238}_{\text{subtr}}(E')} - \frac{\sigma^{239}_{\text{subtr}}(E)}{[\sigma^{238}_{\text{subtr}}(E')]^2}\sigma^{238}_{(\text{n,2n})}(E')\frac{\sigma^{238}_{\text{r-DI}}(E')}{\sigma^{239}_{\text{r-DI}}(E)}\,, \tag{10a}$$

$$\frac{\partial\sigma^{239}_{(\text{n,2n})}(E)}{\partial\sigma^{239}_{\text{f}}(E)} = -\frac{\sigma^{238}_{(\text{n,2n})}(E')}{\sigma^{238}_{\text{subtr}}(E')}\,, \tag{10b}$$

$$\frac{\partial\sigma^{239}_{(\text{n,2n})}(E)}{\partial\sigma^{238}_{\text{f}}(E')} = \frac{\sigma^{239}_{\text{subtr}}(E)\sigma^{238}_{(\text{n,2n})}(E')}{[\sigma^{238}_{\text{subtr}}(E')]^2}\,, \tag{10c}$$

$$\frac{\partial\sigma^{239}_{(n,2n)}(E)}{\partial\sigma^{239}_{(\text{n,n}')}} = -\frac{\sigma^{238}_{(n,2n)}(E')}{\sigma^{238}_{\text{subtr}}(E')}\,, \tag{10d}$$

$$\frac{\partial\sigma^{239}_{(\text{n,2n})}(E)}{\partial\sigma^{238}_{(\text{n,n}')}} = \frac{\sigma^{239}_{\text{subtr}}(E)\sigma^{238}_{(\text{n,2n})}(E')}{[\sigma^{238}_{\text{subtr}}(E')]^2}\,, \tag{10e}$$

$$\frac{\partial\sigma^{239}_{(\text{n,2n})}(E)}{\partial\sigma^{238}_{(\text{n,2n})}(E')} = \frac{\sigma^{239}_{\text{subtr}}(E)}{\sigma^{238}_{\text{subtr}}(E')}\,. \tag{10f}$$

To evaluate the error $\delta\sigma^{239}_{(\text{n,2n})}(E)$ we, eventually, use

$$\delta\sigma^{239}_{(n,2n)}(E) = \sqrt{\sum_{\tau}(\frac{\partial\sigma^{239}_{(\text{n,2n})}(E)}{\partial\sigma_{\tau}}\delta\sigma_{\tau})^2}\,. \tag{11}$$

The index τ in (11) runs over all terms presented in Eq. (10).

In order to calculate $\sigma^{238}_{(\text{n,n}')}(E')$ from Eqs. (3,4) adapted for ^{238}U, we make use of the γ transition 211 keV that is not affected by the wraparound background. In Fig. 6, we present the $\sigma_{(\text{n,n}'\gamma)}$ of this transition. The point at the maximum, just below the ^{238}U(n,2n) threshold of 6.18 MeV, was used for the $\sigma_{(\text{n,n}')}$ normalization (4). When we consider a sum of the 228 keV and 278 keV γ transitions in ^{239}Pu, we obtain the (n,2n) cross section presented in Fig. 7. At 11.37 MeV we get 0.489 ± 0.080 b. The overall error is smaller than in the subtraction approach due to the partial cancellation of the leading error coming from the reaction cross section. We observe that in the energy range of 8-12 MeV, we obtain consistent results from both the subtraction and the ratio approach.

We also used the approach described in this section to compute the ^{239}Pu(n,2n) cross section from the Frehaut measurements of the ^{235}U(n,2n). The results are shown in Fig. 8. At 10.39 MeV, we obtained the cross section of 0.503 ± 0.101 b. At 11.37 MeV, we have the cross section of 0.527 ± 0.102 b. We note that we again summed contributions from the 228 keV and 278 keV transition in ^{239}Pu. In this calculation we obtained a cross section that is consistent with those from the subtraction of Section II and from the ratio using ^{238}U. This is to be expected as the subtracted ^{235}U(n,2n) cross section is in good agreement with the Frehaut measurements as shown in Section II.

IV. ENERGY DEPENDENCE OF THE RATIO OF (N,N') CROSS SECTIONS

A key assumption in the evaluations presented in the previous sections was the relation (3). The modeling performed by M. Chadwick using the code GNASH suggest that the ratio $\sigma_{(\mathrm{n,n'})}/\sigma_{(\mathrm{n,n'}\gamma)}$ may be decreasing with energy [8]. Fig. 9 shows the calculated dependence of this ratio for the ^{239}Pu(n,n'γ) transitions given to us by M. Chadwick. Making use of this dependence in our calculation of the $\sigma_{(\mathrm{n,n'})}$ results in a somewhat lower (n,2n) cross section as shown in Fig. 10. The peak value at 11.37 MeV, presented in Table II, is 0.485 ± 0.104 b. In the error computation we did not associated any error with the ratio modeling calculation.

From Fig. 1 we can see that the non-elastic Flap2.2 cross section is only weakly dependent on energy in the energy range of our interest. In order to test the sensitivity of the (n,2n) cross section evaluation on the non-elastic cross section we performed calculations using three constant non-elastic cross sections set equal to 2.98 b, 2.89 b and 2.82 b, respectively. Our obtained (n,2n) cross sections are presented in Fig. 11 and the corresponding peak values are summarized in Table II. We took into account the (n,n') energy dependence obtained by the GNASH code. From the threshold up to about 6.5 MeV, the (n,2n) cross section is fairly insensitive to the choice of the non-elastic potential. For higher energies the sensitivity is substantial and near the peak we observe differences up to 150 mb.

We note that the constant non-elastic cross section equal to 2.98 b is very close to the Flap2.2 non-elastic cross section. Indeed, in almost the whole energy range of our interest the two cross sections provide very similar (n,2n) cross section. However, near the threshold the Flap2.2 gives a significantly smoother and, thus, more physical (n,2n) cross section. We also note that the constant non-elastic cross section equal to 2.89 b is very close to the measured values [9].

V. SIMULTANEOUS SATISFACTION OF SUBTRACTION AND RATIO RELATIONS FOR ^{239}PU, ^{235}U, ^{238}U AND ^{232}TH

In addition to the above techniques to estimate the (n,2n) cross section from the experimental cross section measurements for a given nucleus, we have also consistently and simultaneously solved the subtraction (1) and the ratio (9) relations for four nuclei, ^{239}Pu, ^{235}U, ^{238}U and ^{232}Th at a single energy, $E_n = 11$ MeV. In this exercise we integrated the experimental neutron emission spectra [10,11] to obtain the (n,n') cross section. We assumed that the (n,n') cross sections of the four nuclei were almost identical up to 20-30 mb, as is observed experimentally in Ref. [12]. We used the measured values of the non-elastic cross sections in Ref. [9] as a starting point and also required that the scaling law (2) be satisfied.

The goal is to satisfy the relations (1) and (9) with the above restrictions and with all the cross sections within the experimental limits. As the fission cross sections are determined accurately with only a small error, we keep them fixed. On the other hand, the four (n,2n) cross sections are allowed to vary as well as the non-elastic cross section and a particular (n,n') cross sections, while the remaining three are tight to this one up to 20(30) mb. Thus, we need to determine six variables plus the three small differences. The number of relations to be satisfied is four following from (1) and four from (9), as we decided to relate the odd nuclei to each of the two even-even nuclei. However, it is obvious that once the subtractions

(1) are satisfied, the ratio equations (9) are satisfied automatically as well. Thus, there are only four independent relations.

In Tables III and V, we present two sets of ranges of the individual cross sections, within which we searched for the consistent satisfaction of the subtraction/ratio relations. As pointed out, there are more variables than equations, but some of the variables are rather severely constrained, while the ^{239}Pu(n,2n) cross section is left almost unconstrained. To generate a distribution of the possible solutions, we decided to construct and minimize the following function

$$F = \sum_{A}(\sigma^{A}_{(\mathrm{n,2n})} - \sigma^{A}_{\mathrm{r-DI}} + \sigma^{A}_{\mathrm{f}} + \sigma^{A}_{(\mathrm{n,n'})})^2 + \sum_{\mathrm{odd,even}} (\sigma^{\mathrm{odd}}_{(\mathrm{n,2n})} - \frac{\sigma^{\mathrm{odd}}_{\mathrm{subtr}}}{\sigma^{\ even}_{\mathrm{subtr}}}\sigma^{\mathrm{even}}_{(\mathrm{n,2n})})^2\,. \tag{12}$$

We randomly generate the starting configurations within the ranges given in Tables III or V and use the CERN library program MINUIT to minimize F. This program performs variations of the parameters within the set limits and finds the minima for which $F = 0$. The distribution of the ^{239}Pu(n,2n) solutions for 30 000 starting configurations within the ranges given in Table III is shown in Fig. 12 and the average values with the statistical errors are presented in Table IV. The results corresponding to the starting ranges of Table IV are presented in Table V and Fig. 13. We used 3000 starting configurations in this case We note that the average values did not change when we varied the number of starting configurations.

From Figs. 12 and 13, it is apparent that the requirement of simultaneous satisfaction of the subtraction equations restricts the possible ranges of the various cross sections. For example, the most important ^{239}Pu(n,2n) cross section never exceeds 0.38 b. No smaller solution then about 0.20 b was obtained, but such a small value results only from very special combination of other cross sections like $\sigma_{\mathrm{r-DI}} \approx 2.7$ b and ^{238}U(n,2n) cross section at its lower limit. As the distribution of the ^{239}Pu(n,2n) cross section solutions is skewed, we computed the median value, 0.339 b, and the range with 66% of solutions, 0.284 b - 0.378 b. The corresponding values for the ^{235}U(n,2n) cross section are the median of 0.811 b and the range of 0.763 b - 0.841 b.

The results of this approach differs from the results of Sections II-III largely because the reaction cross section determined with this self-consistent approach is ≈100 mb smaller than obtained with Flap 2.2.

VI. SUMMARY

We evaluated the (n,2n) cross section of ^{239}Pu and ^{235}U using the subtraction and ratio approaches. We were able to obtain reasonable consistency of the obtained 239Pu(n,2n) from the subtraction and the ratio that relates this cross section to that of ^{238}U. The maximum, though, is about 100 mb too high compared to Frehaut measurements.

When using the new ^{235}U $(\mathrm{n,n'}\gamma)$ data that are free of the wraparound background up to 9.23 MeV, we obtained good agreement with the Frehaut measurements. Also, the ratio that relates ^{239}Pu and ^{235}U is consistent with the above discussed ^{239}Pu results.

It is possible that the discrepancy in the ^{239}Pu (n,2n) cross section will be resolved once the new wraparound free (n,n'γ) data are available. At the same time it should be realized that the simple proportionality relation between the (n,n') and the (n,n'γ) cross section (3) may not be valid in the wide range of energies that we investigated. This is suggested by the GNASH code calculations. Once we utilized the GNASH calculated energy dependence of this ratio, the agreement of the (n,2n) cross section with experiment improved. Another open issue, which could bring agreement between the Frehaut ^{239}Pu measurements and our subtraction and ratio evaluations, is the possibility that a part of the direct processes were not subtracted from the reaction cross section. In order to test the sensitivity to the non-elastic cross section we used three constant non-elastic cross sections. We observed a significant variation of the (n,2n) cross section computed by utilizing the different non-elastic cross sections at the peak region.

The analysis of the cross section data of the four nuclei ^{239}Pu, ^{235}U, ^{238}U and ^{232}Th suggests a significantly smaller value of the ^{239}Pu(n,2n) cross section, while the ^{235}U(n,2n) cross section is in a good agreement with the subtraction and ratio calculation of Sections II and III. It should be stressed that the major difference in the two analysis is in the way, how the (n,n') cross sections were determined. While the former uses a proportionality condition to (n,n'γ) the latter uses the (n,n') cross sections determined from the neutron emission spectra. The non-elastic cross section that we obtained from this analysis was about 2.89 b. It is encouraging that, when we used this value for the non-elastic cross section together with the GNASH energy dependence of the (n,n') cross section ratio, we obtained the (n,2n) cross section that agrees within its errors with that obtained from the four-nuclei analysis.

ACKNOWLEDGMENTS

This work was performed under auspices of the U. S. Department of Energy by the Lawrence Livermore National Laboratory under contract W-7405-ENG-48.

REFERENCES

[1] J. A. Becker and L. Bernstein, private communication (2000).

[2] M. B. Chadwick and P. G. Young, "Calculated Plutonium Reactions for Determining ^{239}Pu(n,2n)^{238}Pu," LAUR-99-2885.

[3] J. D. Anderson, private communication (2000).

[4] H. Vonach, A. Pavlik and B. Strohmaier, Nucl. Sc. Eng. **106**, 409 (1990).

[5] F. S. Dietrich, Optical Model FLAP results (2000).

[6] L. Bernstein, private communication (2000).

[7] W. Younes, private communication (2000).

[8] M. B. Chadwick, private communication (2000).

[9] M. H. MacGregor, R. Booth and W. P. Ball, Phys. Rev. **130**, 1471 (1963).

[10] J. L. Kammerdiener, "Neutron spectra emitted by ^{239}Pu, ^{238,235}U, Nb, Ni, Al and C irradiated by 14 MeV neutrons," Technical Report No. UCRL-51232 (Ph.D. thesis), LLNL (1972).

[11] M. Baba, "Measurements of Prompt Fission Neutron Spectra and Double Differential Neutron Inelastic Scattering Cross Sections for ^{238}U and ^{232}Th," Report JAERI-M-89-143 (1989).

[12] S. M. Grimes, J. D. Anderson and C. Wong, "Odd-Even Effects in Pre-Equilibrium Processes," Technical Report No. UCRL-77438, LLNL (1975).

FIGURES

FIG. 1. Reaction cross section Flap2.2 fitted to the ^{238}U experimental data with the direct excitation of the g.s.b. 2^+ and 4^+ states subtracted together with the experimental fission cross sections of ^{239}Pu and ^{235}U.

FIG. 2. The $\sigma_{(\mathrm{n,n'}\gamma)}$ cross section corresponding to the sum of the two strong transitions, i.e., 228 keV and 278 keV, in ^{239}Pu.

FIG. 3. The ^{239}Pu(n,2n) cross section obtained using the subtraction method.

FIG. 4. The $\sigma_{(\mathrm{n,n'}\gamma)}$ cross section corresponding to the strong 129 keV transition in ^{235}U.

FIG. 5. The ^{235}U(n,2n) cross section obtained using the subtraction method. We compare results for two different $\sigma(n,n')$ calculated using a single γ transition (129 keV) and a sum of the three γ transitions.

FIG. 6. The $\sigma_{(\mathrm{n,n'}\gamma)}$ cross section corresponding to the 211 keV transition in ^{238}U.

FIG. 7. The ^{239}Pu(n,2n) cross section obtained using the ratio method from the ^{238}U(n,2n) experimental cross section.

FIG. 8. The ^{239}Pu(n,2n) cross section obtained using the ratio method from the ^{235}U(n,2n) experimental cross section.

FIG. 9. The energy dependence of the ratio of $\sigma_{(\mathrm{n,n'}\gamma)}/\sigma_{(\mathrm{n,n'})}$ cross sections as calculated using the GNASH code, corresponding to the sum of the two strong transitions, i.e., 228 keV and 278 keV, in ^{239}Pu.

FIG. 10. The ^{239}Pu(n,2n) cross section obtained using the subtraction method with the energy dependence of the $\sigma_{(\mathrm{n,n'}\gamma)}/\sigma_{(\mathrm{n,n'})}$ cross sections as calculated using the GNASH code taken into account.

FIG. 11. The ^{239}Pu(n,2n) cross section obtained using the subtraction method with the energy dependence of the $\sigma_{(\mathrm{n,n'}\gamma)}/\sigma_{(\mathrm{n,n'})}$ cross sections as calculated using the GNASH code taken into account. Results obtained using four different reaction cross sections, Flap2.2 and three constant potentials, are compared.

FIG. 12. *Distribution of the* $\sigma^{239}_{(n,2n)}$ solutions of the subtraction equations of the four studied nuclei, ^{239}Pu, ^{235}U, ^{238}U and ^{232}Th, obtained as discussed in the text. The ranges of the variables and the average values are presented in Tables III and IV, respectively.

FIG. 13. Distribution of the solutions of the subtraction equations of the four studied nuclei, ^{239}Pu, ^{235}U, ^{238}U and ^{232}Th, obtained as discussed in the text. The ranges of the variables and the average values are presented in Tables V and VI, respectively.

TABLES

	$\sigma_{\mathrm{r-DI}}$	σ_{f}	$\sigma_{(\mathrm{n,n'})}$	$\sigma_{(\mathrm{n,2n})}$
^{239}Pu	2.992 ± 0.090	2.235 ± 0.034	0.230 ± 0.034	0.527 ± 0.102
^{235}U	2.959 ± 0.089	1.726 ± 0.026	0.388 ± 0.038	0.844 ± 0.100

TABLE I. The subtracted (n,2n) cross section as well as the non-elastic, fission and (n,n') cross sections of ^{239}Pu and ^{235}U. The cross sections, in b, at energies 11.37 MeV and 11.23 MeV, respectively, are shown.

	$\sigma_{\mathrm{r-DI}}$	σ_{f}	$\sigma_{(\mathrm{n,n'})}$	$\sigma_{(\mathrm{n,2n})}$
^{239}Pu	2.992 ± 0.090	2.235 ± 0.034	0.272 ± 0.040	0.485 ± 0.104
^{239}Pu	2.980 ± 0.089	2.235 ± 0.034	0.286 ± 0.042	0.459 ± 0.105
^{239}Pu	2.890 ± 0.087	2.235 ± 0.034	0.266 ± 0.040	0.389 ± 0.101
^{239}Pu	2.820 ± 0.085	2.235 ± 0.034	0.250 ± 0.037	0.335 ± 0.098

TABLE II. The subtracted (n,2n) cross section as well as the non-elastic, fission and (n,n') cross sections of ^{239}Pu at energies 11.37 MeV. The cross sections, in b, obtained using the Flap2.2 non-elastic cross section and three constant non-elastic cross sections are compared. The energy dependence of the $\sigma_{(\mathrm{n,n'\gamma})}/\sigma_{(\mathrm{n,n'})}$ cross sections as calculated using the GNASH code was taken into account.

	$\sigma_{\mathrm{r-DI}}$	σ_{f}	$\sigma_{(\mathrm{n,n'})}$	$\sigma_{(\mathrm{n,2n})}$
^{239}Pu		2.234	0.290 - 0.400	0.100 - 0.700
^{235}U		1.726	$\sigma^{239}_{(\mathrm{n,n'})} \pm 0.020$	0.700 - 0.900
^{238}U	2.7 - 3.1	0.983	$\sigma^{239}_{(\mathrm{n,n'})} \pm 0.020$	1.414-1.594
^{232}Th		0.305	$\sigma^{239}_{(\mathrm{n,n'})} \pm 0.020$	2.00 - 2.30

TABLE III. The values and ranges, in b, of the various cross sections used in the analysis. The non-elastic cross sections are related by the scaling law as described in the text.

	$\sigma_{\mathrm{r-DI}}$	$\sigma_{(\mathrm{n,n'})}$	$\sigma_{(\mathrm{n,2n})}$
^{239}Pu		0.347 ± 0.036	0.323 ± 0.045
^{235}U		0.347 ± 0.039	0.799 ± 0.040
^{238}U	2.896 ± 0.064	0.359 ± 0.038	1.554 ± 0.038
^{232}Th		0.352 ± 0.039	2.190 ± 0.043

TABLE IV. The average values and statistical errors, in b, of the various cross sections determined from the analysis using the ranges from Table III. The non-elastic cross sections are related by the scaling law as described in the text.

	$\sigma_{\mathrm{r-DI}}$	σ_{f}	$\sigma_{(\mathrm{n,n'})}$	$\sigma_{(\mathrm{n,2n})}$
^{239}Pu		2.234	0.290 - 0.400	0.180 - 0.650
^{235}U		1.726	$\sigma^{239}_{(\mathrm{n,n'})} \pm 0.030$	0.700 - 0.900
^{238}U	2.7 - 3.1	0.983	$\sigma^{239}_{(\mathrm{n,n'})} \pm 0.030$	1.414-1.594
^{232}Th		0.305	$\sigma^{239}_{(\mathrm{n,n'})} \pm 0.030$	2.00 - 2.30

TABLE V. The values and ranges, in b, of the various cross sections used in the analysis. The non-elastic cross sections are related by the scaling law as described in the text.

	$\sigma_{\mathrm{r-DI}}$	$\sigma_{(\mathrm{n,n'})}$	$\sigma_{(\mathrm{n,2n})}$
^{239}Pu		0.344 ± 0.036	0.331 ± 0.044
^{235}U		0.347 ± 0.042	0.804 ± 0.039
^{238}U	2.901 ± 0.065	0.363 ± 0.040	1.556 ± 0.036
^{232}Th		0.354 ± 0.042	2.193 ± 0.043

TABLE VI. The average values and statistical errors, in b, of the various cross sections determined from the analysis using the ranges from Table V. The non-elastic cross sections are related by the scaling law as described in the text.

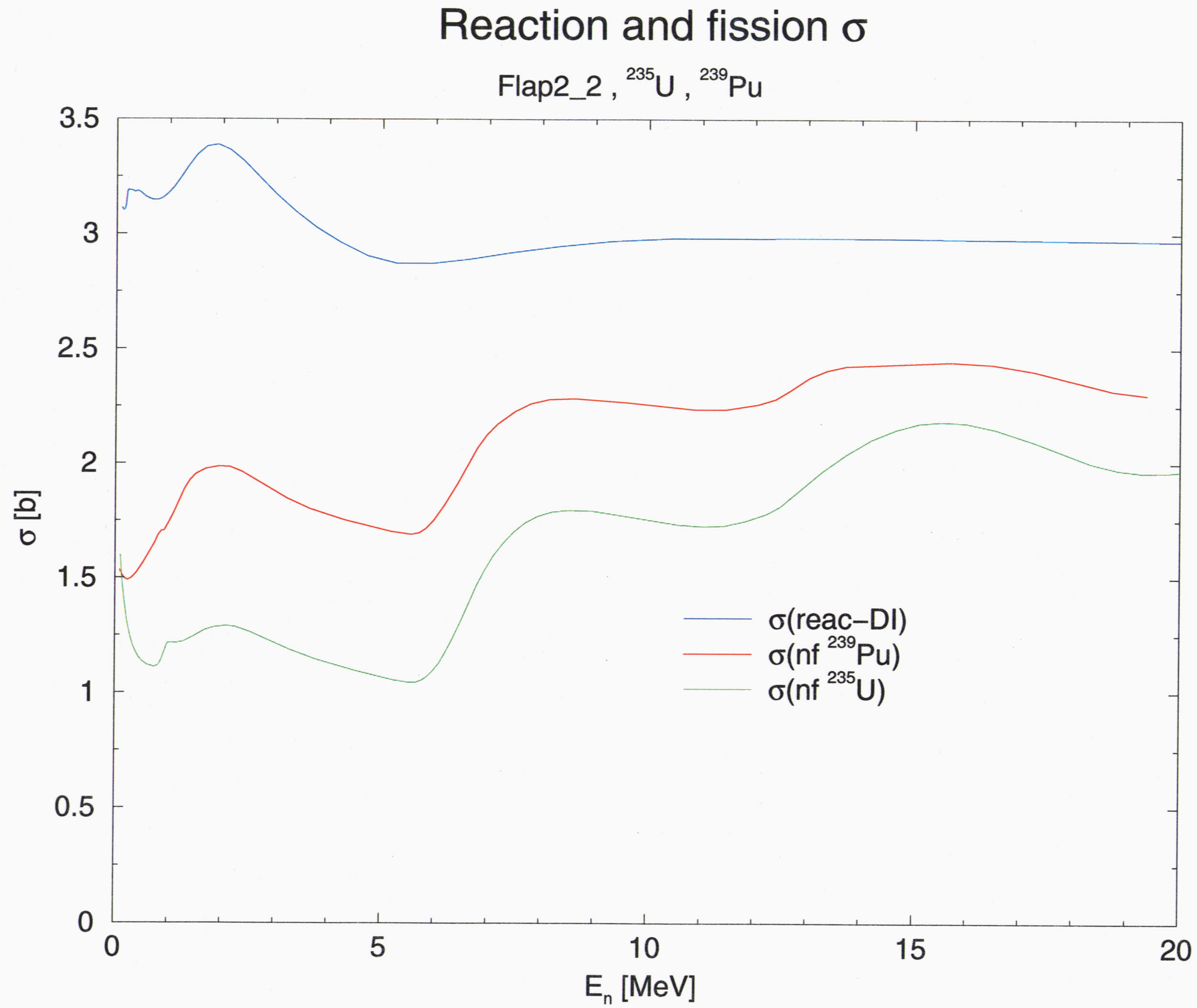
Reaction and fission σ
Flap2_2 , 235U , 239Pu
σ [b]
E_n [MeV]
σ(reac−DI)
σ(nf 239Pu)
σ(nf 235U)
0
0.5
1
1.5
2
2.5
3
3.5
0
5
10
15
20

Fig. 1

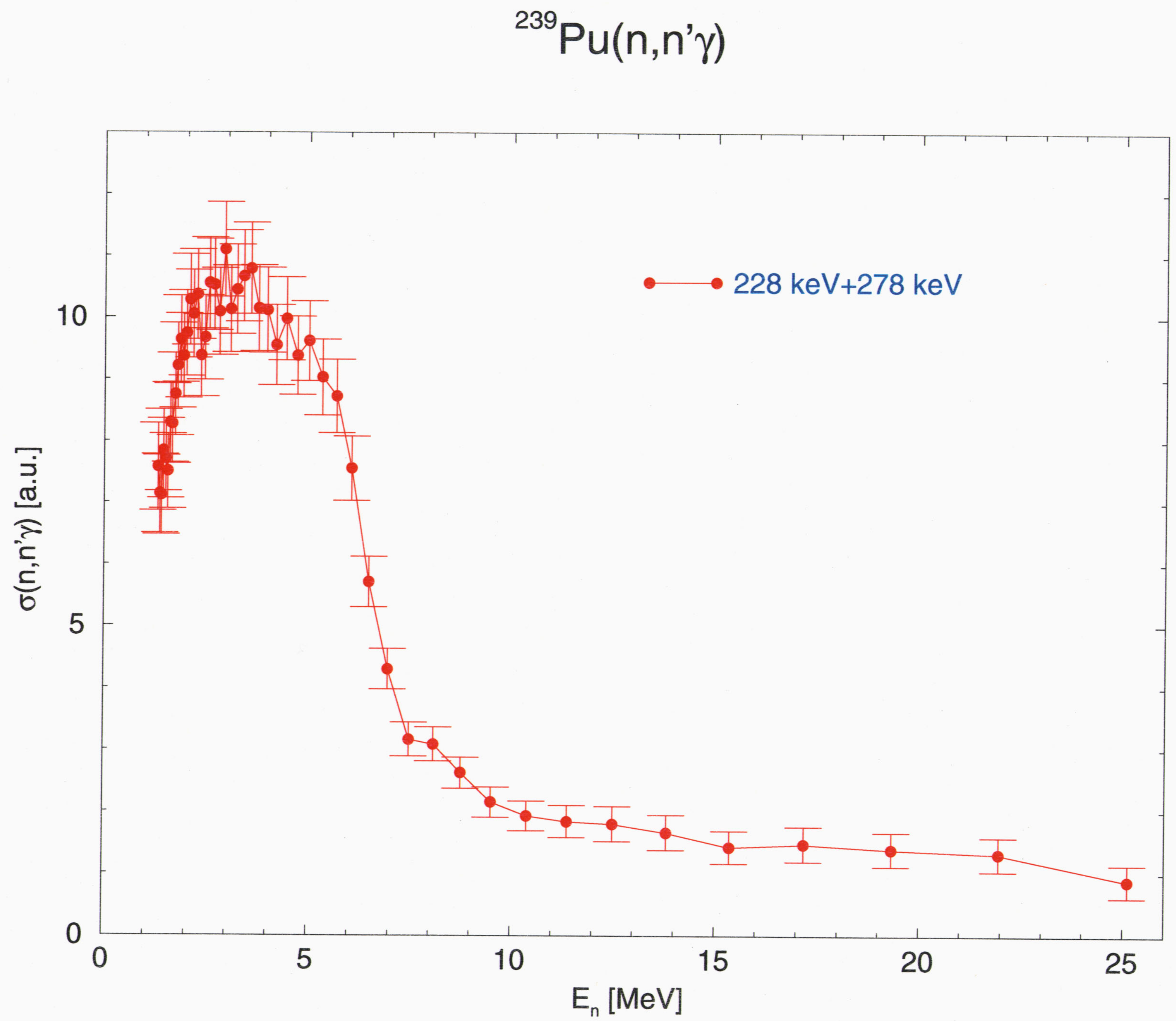

Fig. 2

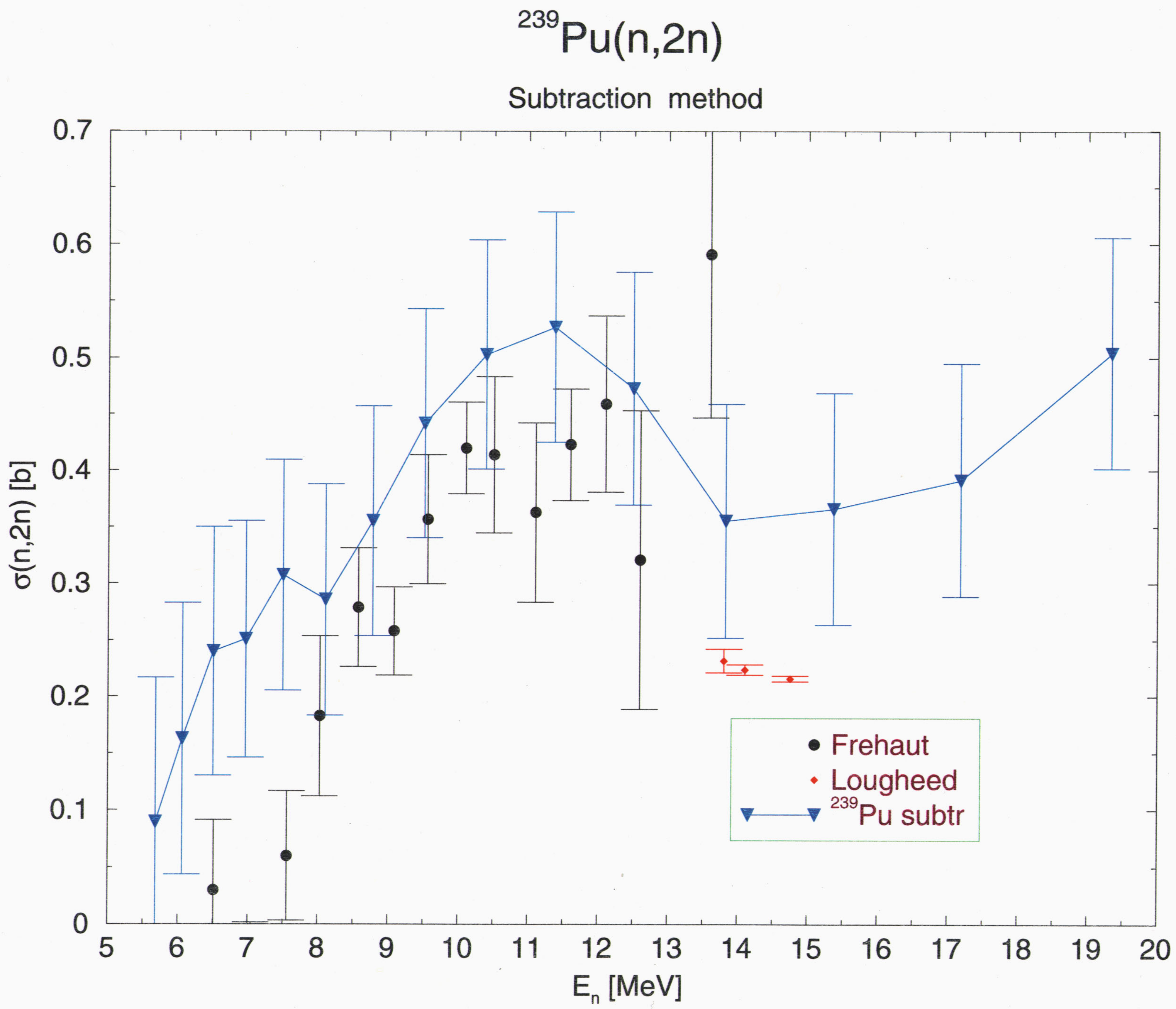

239Pu(n,2n)
Subtraction method
σ(n,2n) [b]
E_n [MeV]
0
0.1
0.2
0.3
0.4
0.5
0.6
0.7
5
6
7
8
9
10
11
12
13
14
15
16
17
18
19
20
Frehaut
Lougheed
239Pu subtr

Fig. 3

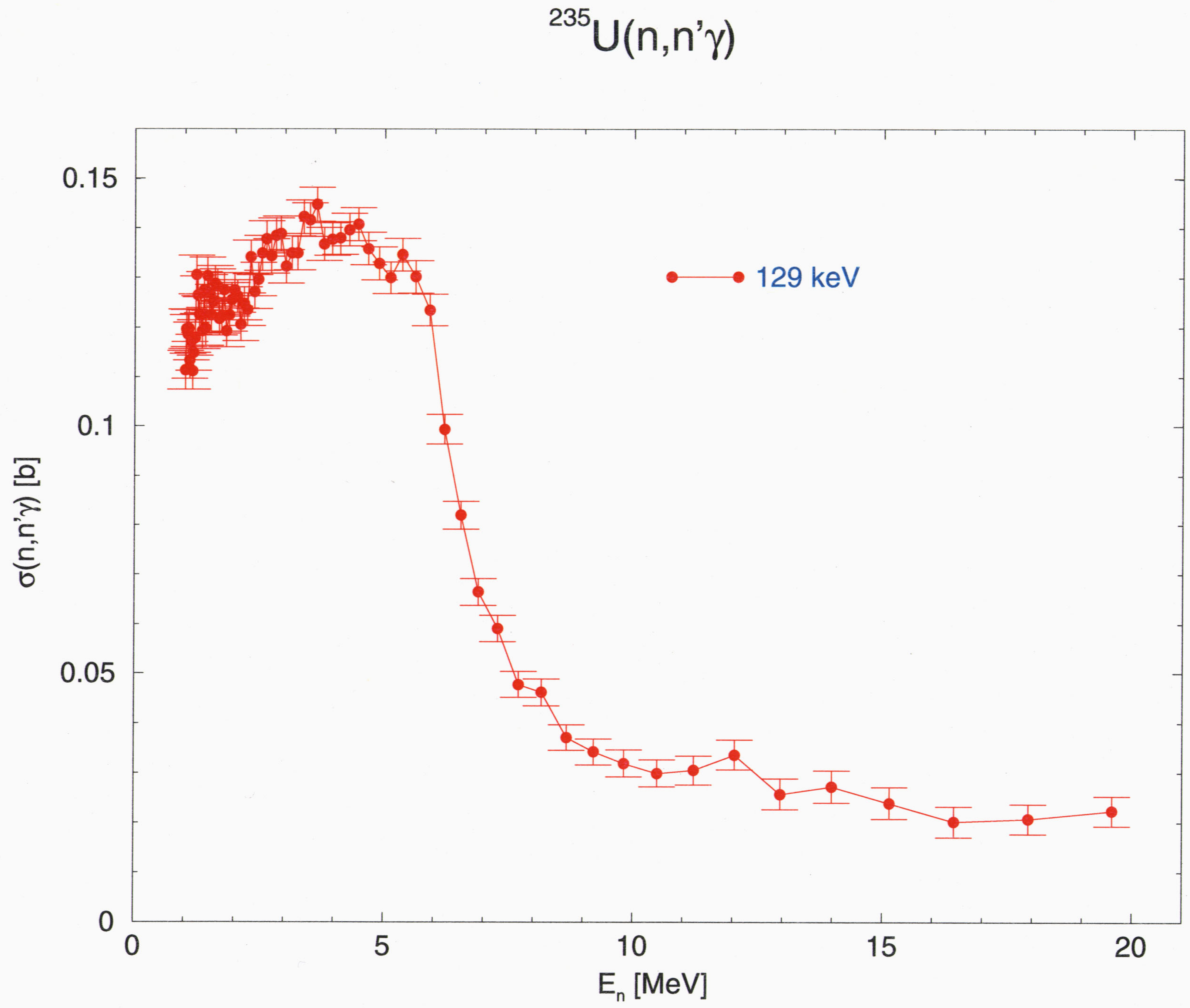

Fig. 4

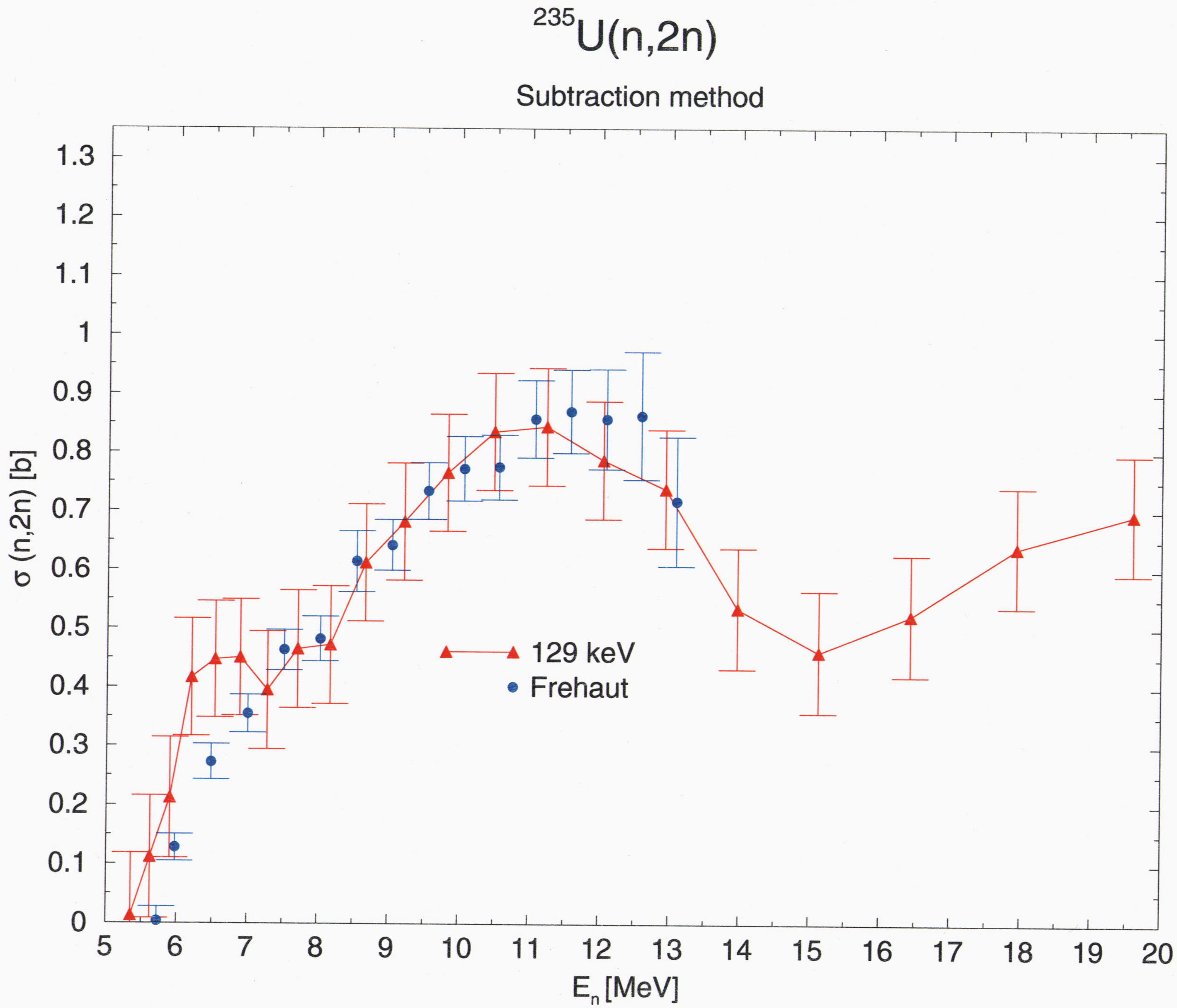

Fig. 5

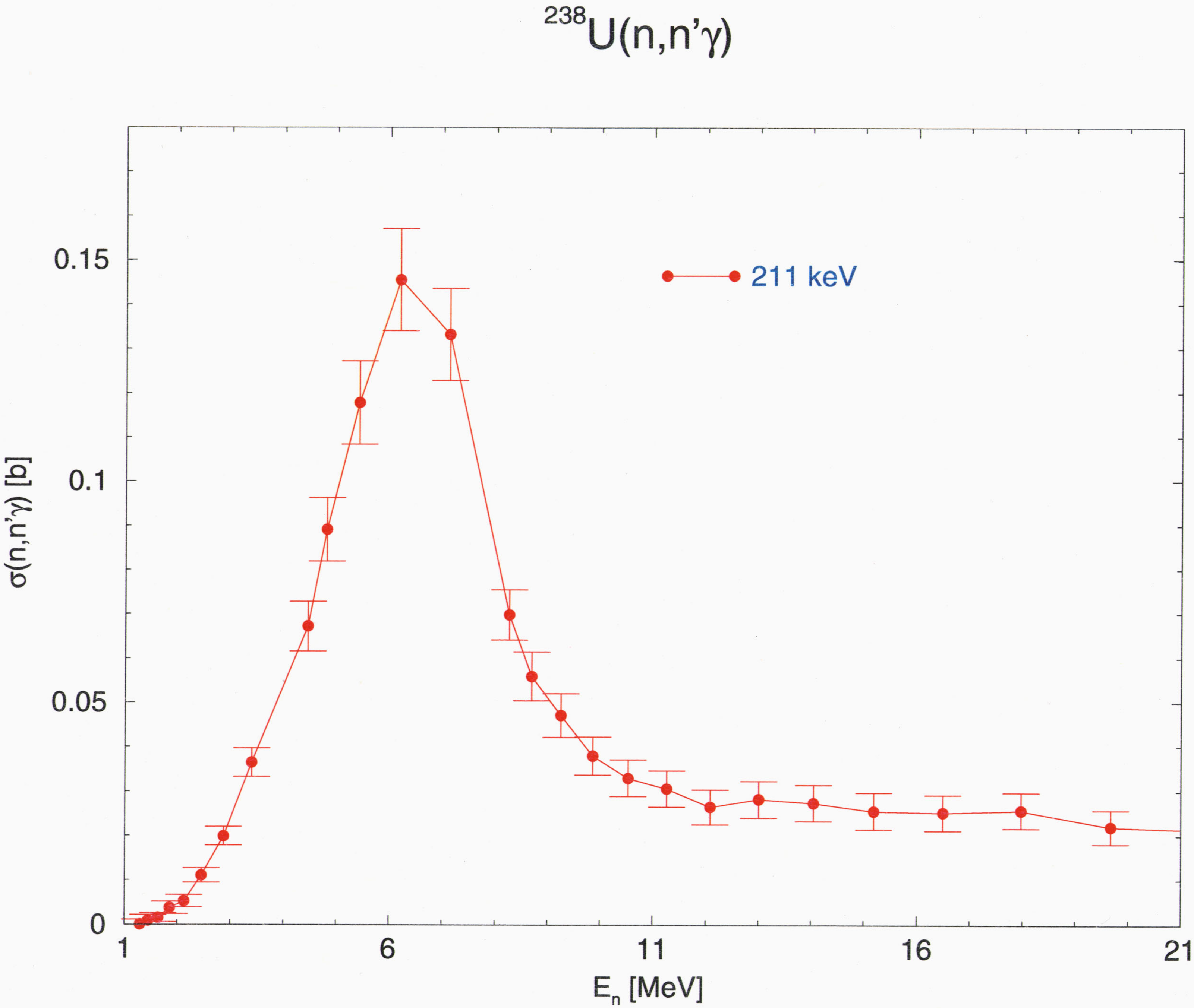

$^{238}U(n,n'\gamma)$
211 keV
$\sigma(n,n'\gamma)$ [b]
0.15
0.1
0.05
0
1
6
11
16
21
E_n [MeV]

Fig. 6

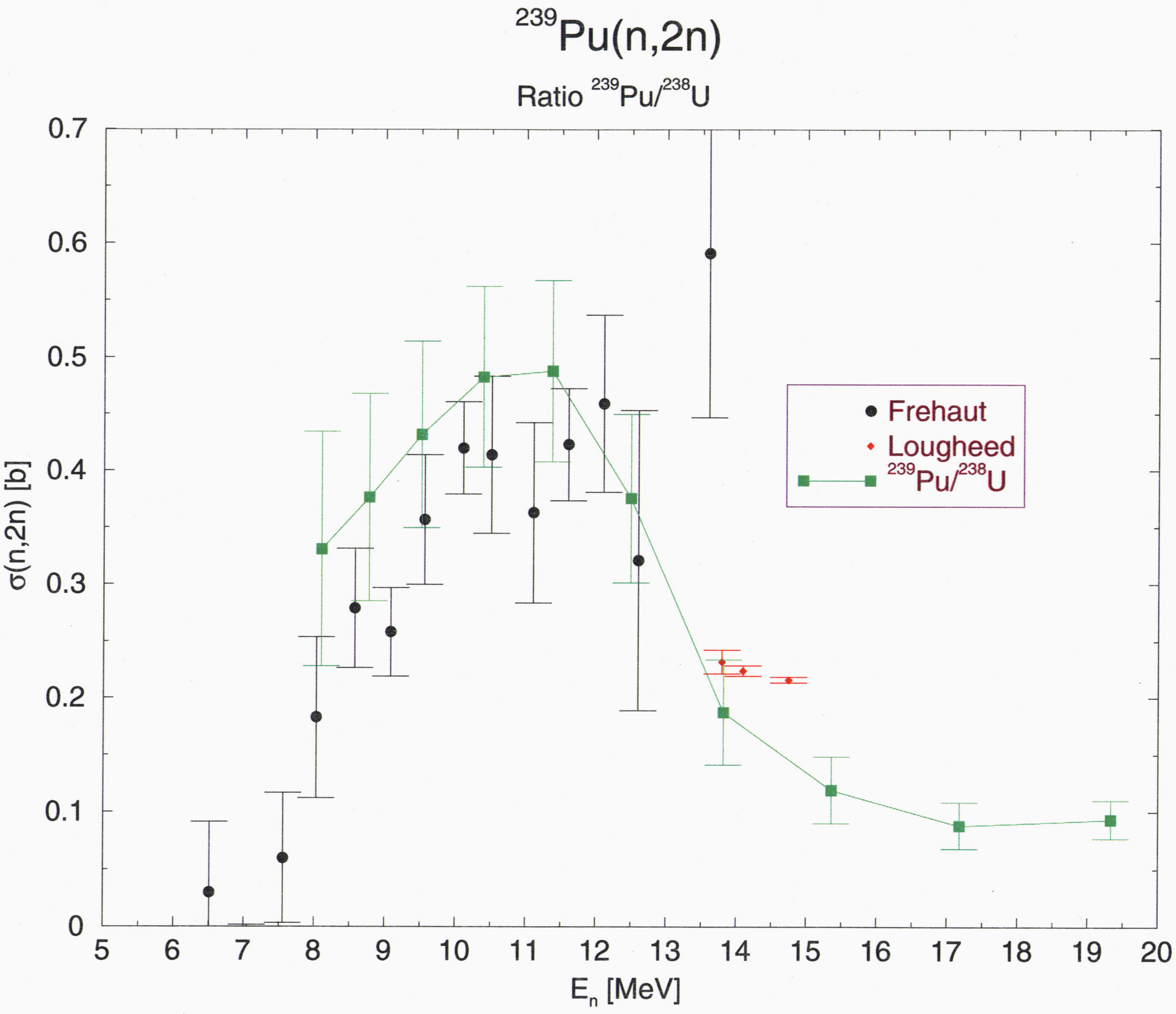
239Pu(n,2n)
Ratio 239Pu/238U
σ(n,2n) [b]
En [MeV]
Frehaut
Lougheed
239Pu/238U
0.7
0.6
0.5
0.4
0.3
0.2
0.1
0
5
6
7
8
9
10
11
12
13
14
15
16
17
18
19
20

Fig. 7

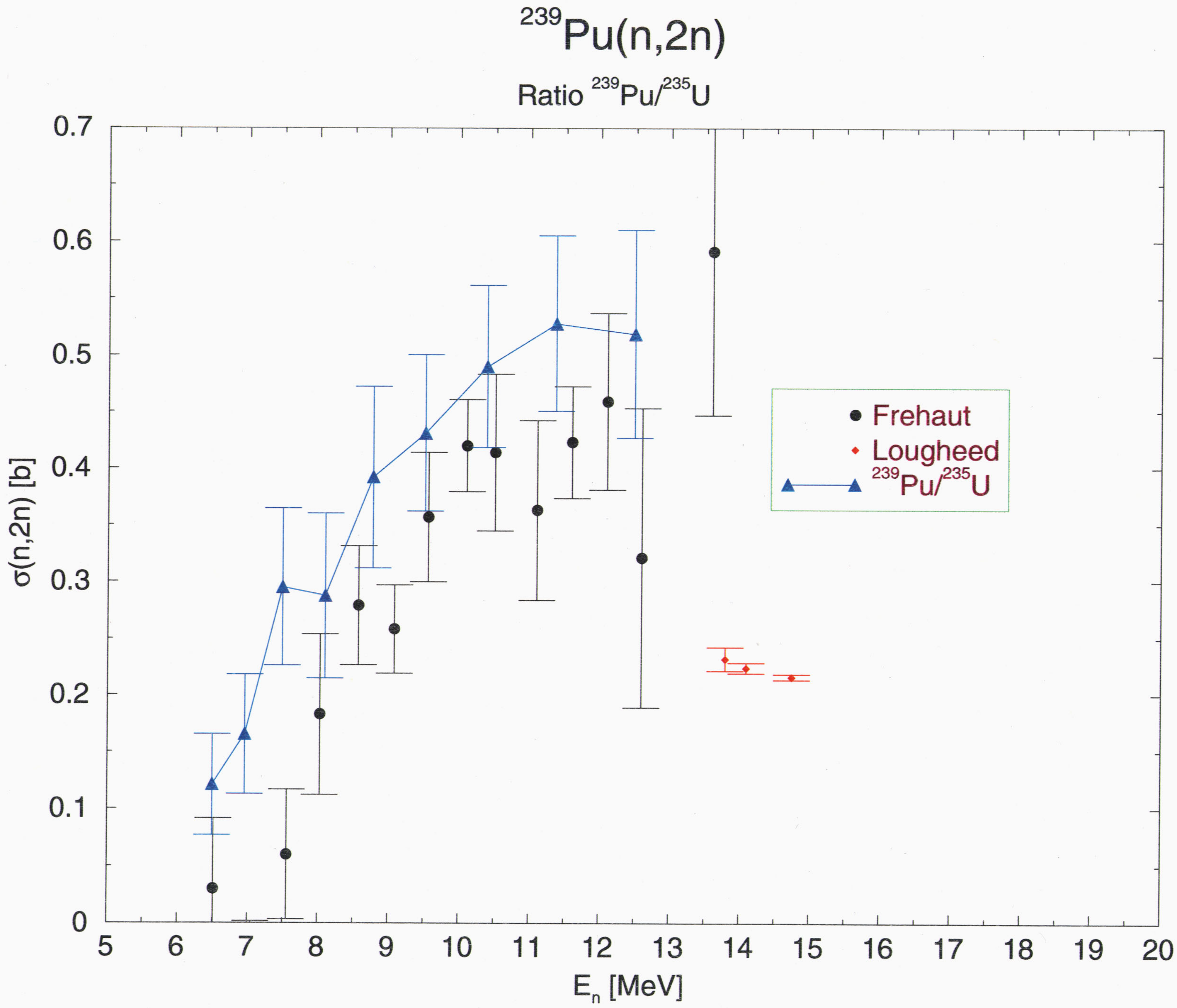
$^{239}Pu(n,2n)$
Ratio $^{239}Pu/^{235}U$
σ(n,2n) [b]
E_n [MeV]
0
0.1
0.2
0.3
0.4
0.5
0.6
0.7
5
6
7
8
9
10
11
12
13
14
15
16
17
18
19
20
Frehaut
Lougheed
$^{239}Pu/^{235}U$

Fig. 8

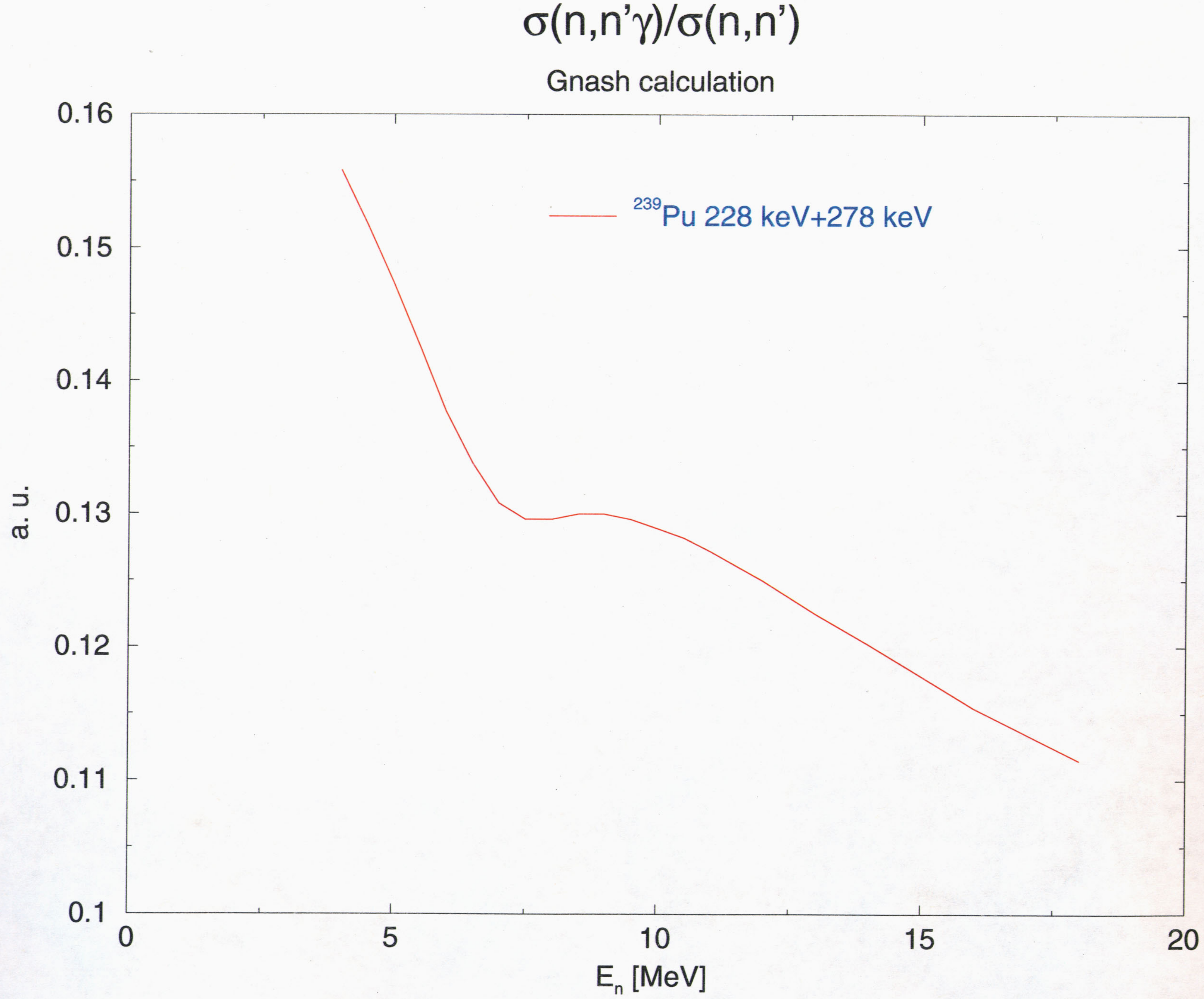
σ(n,n'γ)/σ(n,n')
Gnash calculation
0.16
0.15
0.14
0.13
0.12
0.11
0.1
a. u.
0
5
10
15
20
E_n [MeV]
239Pu 228 keV+278 keV

Fig. 9

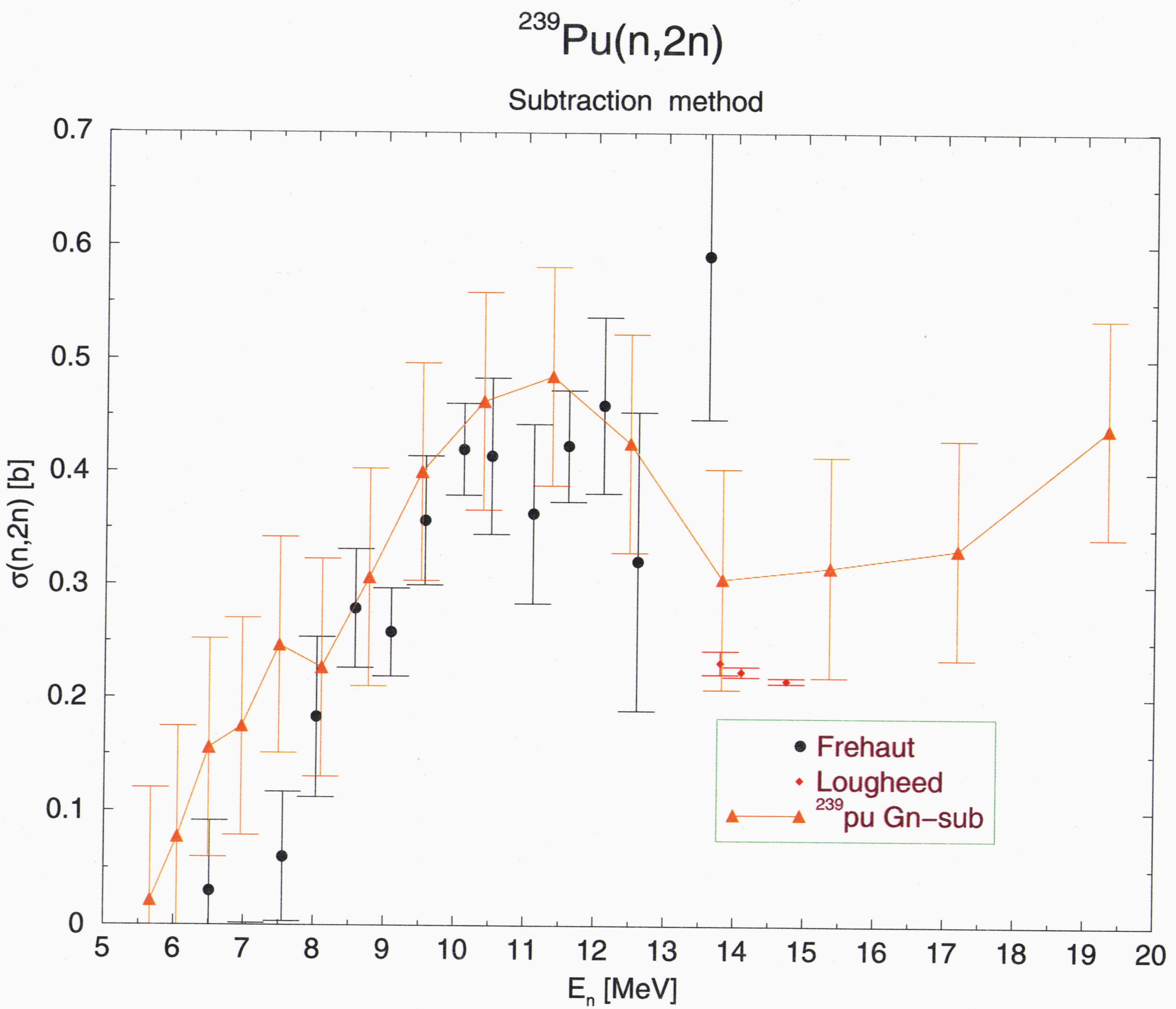
239Pu(n,2n)
Subtraction method
σ(n,2n) [b]
E_n [MeV]
Frehaut
Lougheed
239pu Gn-sub

Fig. 10

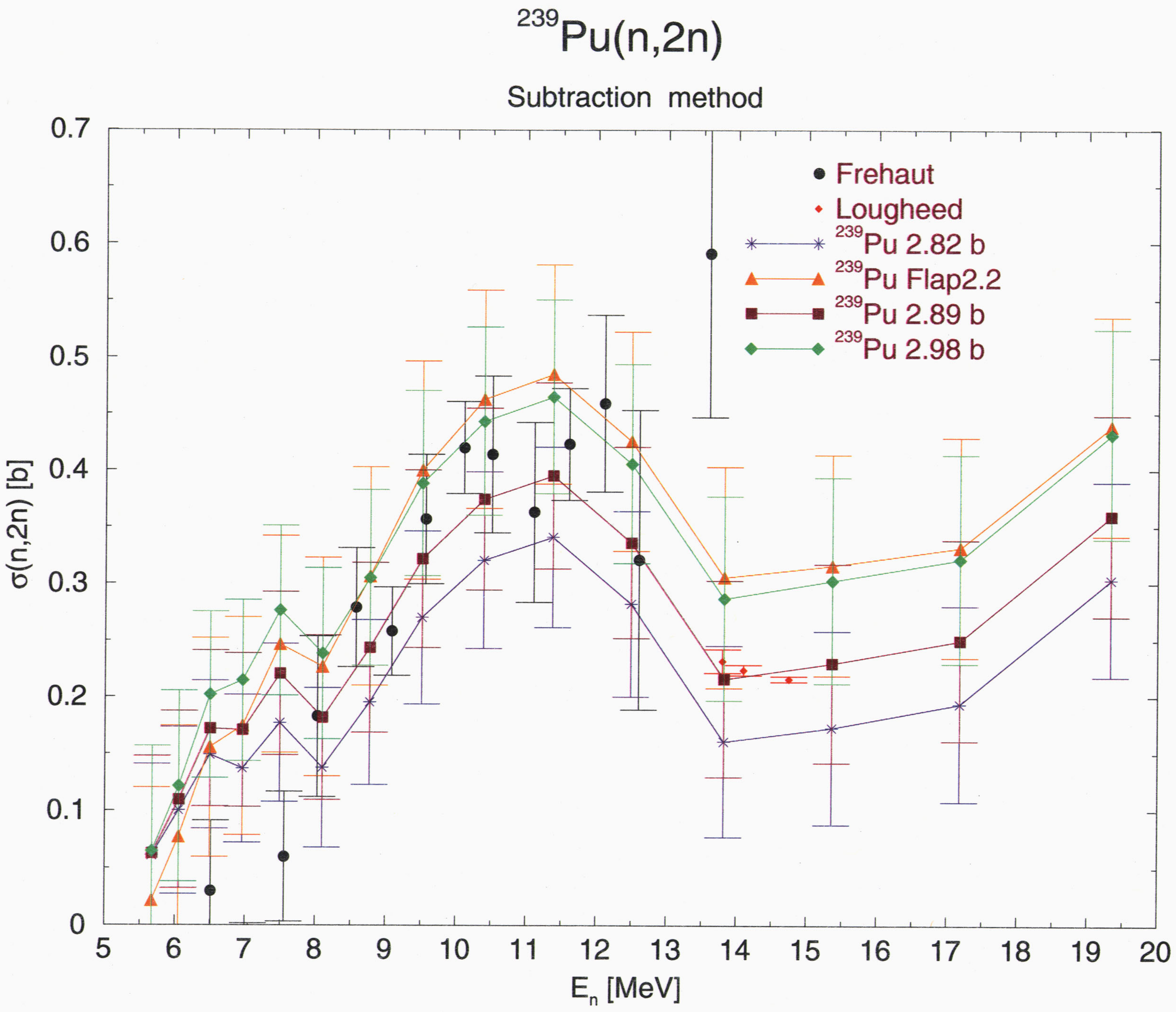

^{239}Pu(n,2n)
Subtraction method
σ(n,2n) [b]
0.7
0.6
0.5
0.4
0.3
0.2
0.1
0
5
6
7
8
9
10
11
12
13
14
15
16
17
18
19
20
E_n [MeV]
Frehaut
Lougheed
^{239}Pu 2.82 b
^{239}Pu Flap2.2
^{239}Pu 2.89 b
^{239}Pu 2.98 b

Fig. 11

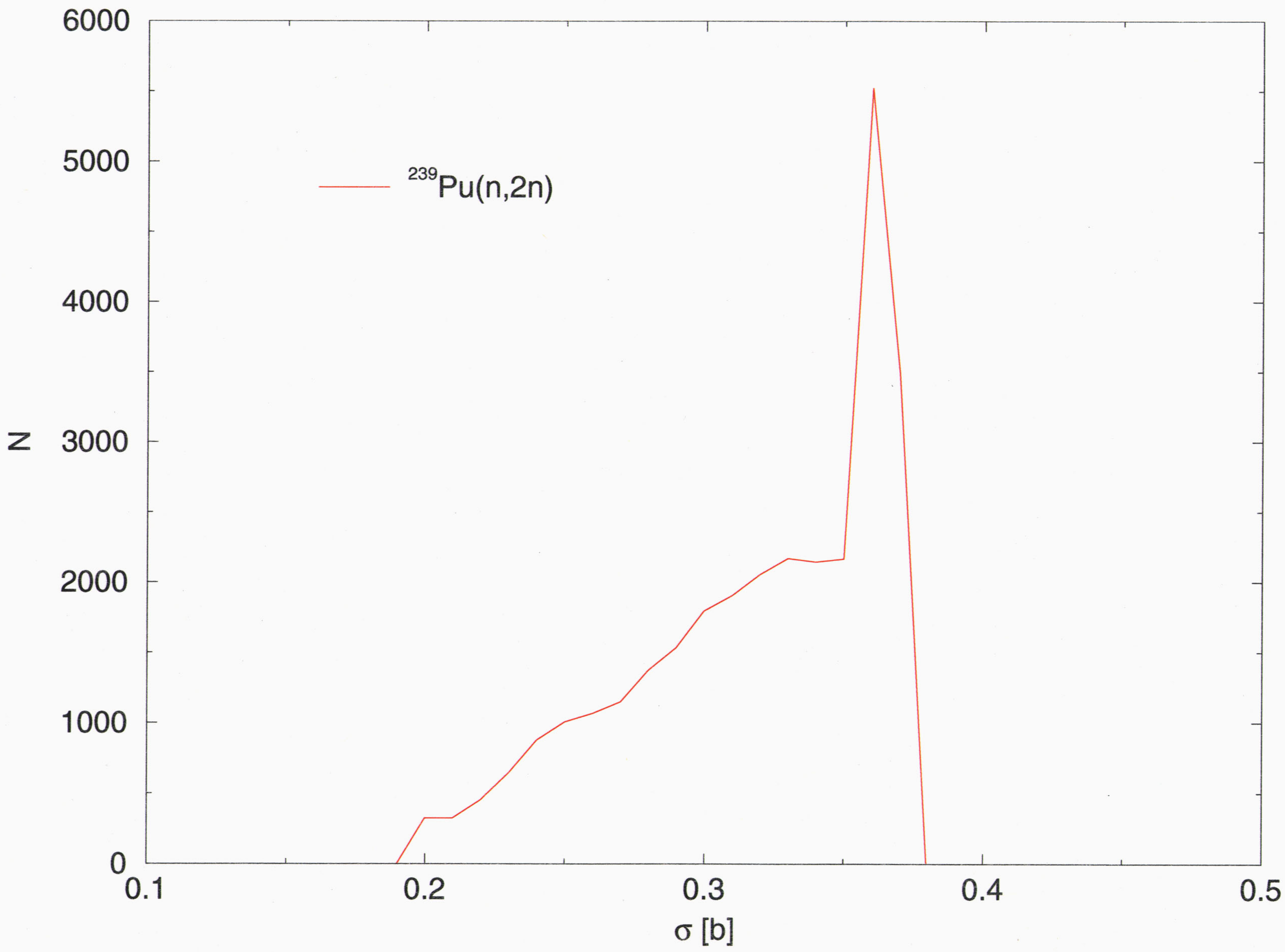

Fig. 12

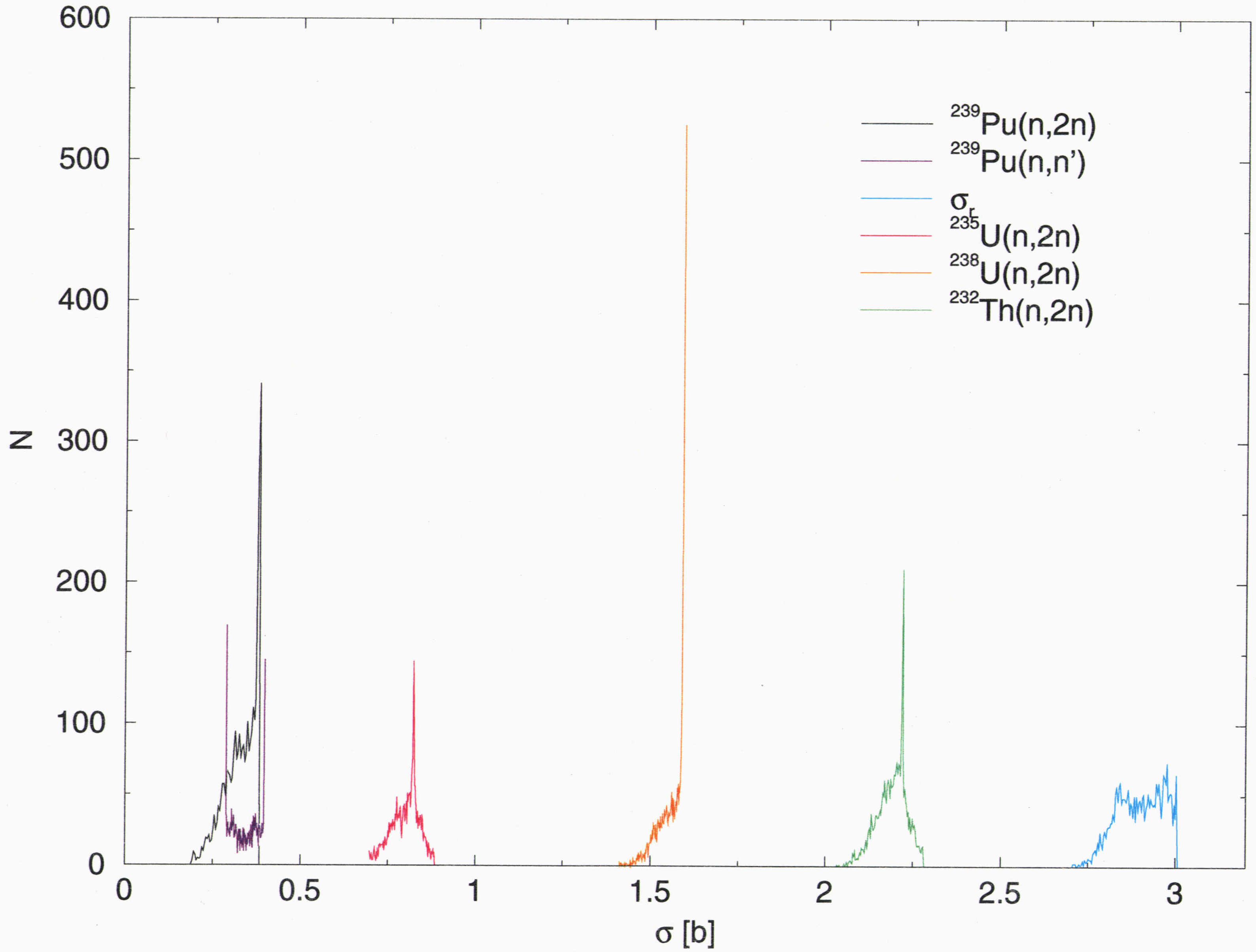
600
500
400
300
200
100
0
N
0
0.5
1
1.5
2
2.5
3
σ [b]
239Pu(n,2n)
239Pu(n,n')
σr
235U(n,2n)
238U(n,2n)
232Th(n,2n)

Fig. 13